doi.org/10.36721/PJPS.2026.39.5.REG.15336.1

Esketamine and postoperative cognitive dysfunction in aged mice: Role of the SIRT3/AMPK/mTOR pathway

Yunfei Wang[1#], Tao Cui[2#], Jiafang Wang[1], Li Zhang[1], Zhe Ding[4] and Lu Zou[3]*

[1]Department of Anesthesiology, Wuhan No.1 Hospital, Wuhan City, Hubei Province, China
[2]Anesthesiology Department, The Third People's Hospital of Hubei Province, Hubei Province, China
[3]Department of Anesthesiology, Changzhou Hospital of Traditional Chinese Medicine, Changzhou City, Jiangsu Province, China
[4]Department of Painology, Wuhan No.1 Hospital, Wuhan City, Hubei Province, China

Abstract: **Background**: Postoperative cognitive dysfunction (POCD) frequently occurs after surgery in older patients. **Objectives**: To investigate whether esketamine (Esk) mitigates POCD in aged mice by regulating the sirtuin 3 (SIRT3)/AMP-activated protein kinase (AMPK)/mammalian target of rapamycin (mTOR) pathway. **Methods**: In this study, a POCD mouse model was established via modified abdominal exploration laparotomy (n=10/group) and an LPS-induced inflammatory model of BV-2 cells was constructed (n=5/group). The effects of Esk on behavior and hippocampal tissue injury in POCD mice were observed through Morris water maze test and pathological staining. The content of inflammatory cytokines, oxidative stress and mitochondrial function-related indicators were detected using kits. Western blot analysis detected SIRT3/AMPK/mTOR pathway and M1 polarization markers levels. **Results**: POCD mice showed significantly reduced spatial learning and memory abilities, while Esk improved the spatial memory abilities (P<0.05). Esk also alleviated brain tissue damage, neuroinflammation and oxidative stress, inhibited M1 polarization of microglia and improved mitochondrial function in POCD mice. In BV-2 cells, Esk rescued LPS-induced viability reduction, inflammatory factor release and M1 polarization. Mechanistically, Esk regulated SIRT3/AMPK/mTOR pathway, while silencing SIRT3 weakened the neuroprotective effects of Esk. **Conclusion**: Esk appears to regulate SIRT3/AMPK/mTOR pathway to inhibit neuroinflammation and improve mitochondrial dysfunction, thereby mitigating POCD in aged mice.

Keywords: Esketamine; Mitochondrial dysfunction; Neuroinflammation; Postoperative cognitive dysfunction; SIRT3/AMPK/mTOR pathway

Submitted on 09-10-2025 – Revised on 21-11-2025 – Accepted on 11-12-2025

INTRODUCTION

Postoperative cognitive dysfunction (POCD) frequently occurs in older patients after surgery, which causes a decline in memory, learning ability and perception, severely affecting the patient's postoperative quality of life (Anand *et al.*, 2024; Varpaei *et al.*, 2024). Although research on POCD is increasing, its potential pathophysiological mechanisms are yet to be clarified and targeted treatment options are insufficient (Bhushan *et al.*, 2021; Peng *et al.*, 2023; Nešković *et al.*, 2025). Numerous research efforts indicate that mitochondrial dysfunction, neuroinflammation and oxidative stress are crucial parts of its pathogenesis (Yang *et al.*, 2022; Liu *et al.*, 2025a). Neuroinflammation can stimulate microglia, causing them to polarize to the proinflammatory M1 type and release large amounts of inflammatory factors, which in turn damage neurons (Rump and Adamzik, 2022; Wang *et al.*, 2023). At the same time, impaired mitochondrial function caused abnormal energy metabolism and triggers oxidative stress, further damaging cell structure and function impairing neurocognitive functions (Ying *et al.*, 2024). Thus, clarifying the exact mechanisms of POCD and developing effective treatment strategies is urgent.

Recently, the clinical value of esketamine (Esk) has attracted considerable attention. As the S-enantiomer of ketamine, Esk has similar pharmacological effects to ketamine (Shoib *et al.*, 2022). Both can exert effects such as alleviating depression, producing sedation and reducing pain by influencing the release of neurotransmitters and receptor activation in central nervous system (Bahji *et al.*, 2022; Feeney and Papakostas, 2023). Pharmacokinetic studies have shown that Esk has the advantage of rapid absorption, high absolute bioavailability and high clearance efficiency (Jonkman *et al.*, 2017; Pavlidi *et al.*, 2021; Vekhova *et al.*, 2025). Numerous investigations have demonstrated that Esk exhibits neuroprotective properties and can alleviate neurological damage induced by traumatic brain injury, cerebral ischemia/reperfusion injury and sepsis-associated encephalopathy (Tang *et al.*, 2023; Li *et al.*, 2024; Gao *et al.*, 2025). Critically, its neuroprotective mechanisms directly target POCD's core pathologies, Esk suppresses neuroinflammation, regulates apoptosis and improves mitochondrial function (Han *et al.*, 2023; Ma *et al.*, 2025). For example, Esk drives microglial polarization to the anti-inflammatory M2 phenotype to alleviate neuronal injury in cerebral ischemia/reperfusion (Gao *et al.*, 2025). However, the effects of Esk on POCD in aged mice and its mechanism of action have not been well studied.

**Corresponding author:* e-mail: zl3552468@hotmail.com

The Sirtuin 3 (SIRT3)/AMP-activated protein kinase (AMPK)/mammalian target of rapamycin (mTOR) signaling pathway is closely implicated in POCD progression (Li *et al.*, 2022). SIRT3 participates in processes like oxidative stress defense, energy metabolism and apoptosis regulation (Guo *et al.*, 2021; Zhou *et al.*, 2022). As a serine/threonine kinase, AMPK is responsible for maintaining energy homeostasis, reducing inflammation and inhibiting oxidative stress (Trefts and Shaw, 2021). Excessive activation of mTOR is linked to pathological conditions such as neuroinflammation and neuronal damage (Xu *et al.*, 2021; Ravizza *et al.*, 2024). In POCD mice, upregulating SIRT3 can enhance cognitive function, increase AMPK phosphorylation levels and reduce mTOR phosphorylation levels (Li *et al.*, 2022), implying that targeting and regulating SIRT3/AMPK/mTOR pathway may be a potential treatment approach for POCD. Notably, Esk has been shown to modulate the AMPK/mTOR pathway to alleviate oxidative stress and neuronal damage in traumatic brain injury (Tang *et al.*, 2023). Nonetheless, it remains uncertain whether Esk can alleviate POCD progression by regulating the SIRT3/AMPK/mTOR pathway.

Based on the aforementioned research background, we hypothesize that Esk alleviates the progression of POCD by modulating the SIRT3/AMPK/mTOR pathway. This study focuses on the impact of Esk on cognitive function, neuroinflammation, mitochondrial dysfunction and oxidative stress in elderly mice with POCD and explores whether it exerts its effects through the SIRT3/AMPK/mTOR pathway. This study aims to establish a theoretical foundation for the clinical use of Esk and the development of treatment strategies for POCD.

MATERIALS AND METHODS

Experimental animals and treatment

18-month-old C57BL/6 mice were from Saiye Biotechnology Co., Ltd. (Suzhou, Jiangsu, China), raised in a standard indoor clean environment with 20±2°C, humidity of 50%-60% and a 12-hour light/dark cycle. The cages used in the experiment were disinfected regularly to ensure the cleanliness and safety of the feeding environment.

After seven days of adaptation to the environment, the mice were randomly assigned using a random number table to control (Con) group, POCD group and POCD + Esk group, with each group consisting of 10 mice. Experimental group information was coded by independent personnel. To minimize bias, a double-blind approach was adopted. All the researchers involved in animal breeding, model construction, behavioral assessment and pathological section staining were unaware of the grouping situation. Before modeling, mice from each group underwent water maze training, completing four sessions daily for five consecutive days. Mice with mental retardation or inability to swim were excluded to guarantee an absence of statistical disparity in cognitive function across the groups. Based on previous research (Xu *et al.*, 2024), mice in the POCD +Esk group received intraperitoneal injections of Esk (5 mg/kg, Jiangsu Hengrui Medicine Co., Ltd., China) for 7 consecutive days starting from 3 days before surgery. The mice in the POCD group and the POCD + Esk group underwent anesthesia through the inhalation of 1.5 % sevoflurane (mixed with oxygen, 2 L/min). The limbs of the mice were fixed, the hair in the abdominal operation area was cut off, disinfected with iodophor and the middle skin was cut. The length of the incision was about 1-2cm, revealing the abdominal white line. The peritoneum was cut and inserted into the abdominal cavity with scissors and then the abdominal organs were explored with tweezers and the peritoneum and skin were sutured. The operation was performed under anesthesia for about 1 h. Mice in the Con group received continuous inhalation of 1.5% sevoflurane (mixed with oxygen at 2 L/min) for 1 hour, along with an intraperitoneal injection of an equal volume of saline (solvent) but did not undergo exploratory laparotomy. The mice were put back into the cage after the natural awakening of the mice. The whole operation process strictly maintained the principle of aseptic operation (Li *et al.*, 2025). This study was approved by the Department of Anesthesiology, Wuhan No.1 Hospital Ethics Committee [(2024)33] and strictly adhered to the Guidelines for Ethical Review of Laboratory Animal Welfare and the ARRIVE guidelines.

Morris water maze test

Three days following the establishment of the POCD model, the directional navigation experiment was performed to determine the escape latency of the mice (Liu *et al.*, 2021a). The water maze system (Noldus, EthoVision XT 19) includes a 100 cm-diameter cylindrical pool and a 10 cm-diameter circular platform. The pool is divided into four quadrants of 1, 2, 3 and 4 and the platform is positioned in center of quadrant 1. The experiment was conducted once a day for 5 consecutive days. The mice were placed in water from the same point in the four quadrants in turn during the experiment and escape latency was documented as the duration from the mouse entering the water to finding the hidden platform. After finding the hidden platform, the mice could stay on the platform for 15 s. When mice did not find the hidden platform within 60 s, they were manually assisted onto the hidden platform for 15 s and the average escape latency of the four quadrants per day was documented as the escape latency of the day. On the 7th day after operation, a space exploration test was conducted to assess the activity time of the target quadrant. After removing the hidden platform, each mouse was positioned into the quadrant outside the target quadrant and allowed to cross the target quadrant within 60 s. The total time the mouse spent in the target quadrant and the number of times it crossed platform location were documented (Xu

et al., 2024). To avoid behavioral assessment bias, establish standardized behavioral assessment protocols in advance, ensuring consistent testing conditions (temperature, lighting, noise) and equipment parameters (tank diameter, platform placement, camera angles) throughout the entire process. The core metrics of the Morris water maze (escape latency, platform crossing times and time spent in the target quadrant) were automatically collected and calculated using a video tracking analysis system, thereby eliminating human subjective judgment errors. After the behavioral test, mice were euthanized using pentobarbital sodium (150 mg/kg). Complete brain tissues were then dissected using surgical scissors and collected for subsequent experimental analyses.

TUNEL staining

Mouse brain tissue was completely removed on ice and transferred to 4% paraformaldehyde (P885233, Macklin, Shanghai, China) overnight (Ding *et al.*, 2022). The brain tissue was dehydrated with gradient ethanol (100%, 95%, 75% and 50%). The dehydrated brain tissue was transparentized in xylene (X821391, Macklin) and subsequently embedded with paraffin and prepared into 4μm sections. After xylene dewaxing, it was placed in gradient ethanol for rehydration, 5 min each time. Sections were exposed to 0.1% Triton X-100 (T824275, Macklin) at 25°C for 2 min to increase permeability. 20μg/mL of DNase-free protease K (ST532, Beyotime, Shanghai, China) was added dropwise onto the sections, followed by a 30-minute reaction at 25°C and washed with PBS. After that, TUNEL detection solution (C1086, Beyotime) was applied to the sections and left to incubate for 1.5 h in a dark environment. AntiFade Mounting Medium (HY-K1047, MedChemExpress, Monmouth Junction, NJ, USA) with DAPI was used to seal the slice. Under DM3000 fluorescence microscope (Leica, Heidelberg, Germany), five random fields of view were selected for observation and photography. Fluorescence intensity of the sections was quantified using Image J software (version 1.46, Wayne Rasband, National Institute of Mental Health, USA), with the average fluorescence intensity of TUNEL measured under identical exposure parameters. Background fluorescence intensity was subtracted prior to intergroup comparisons.

Hematoxylin and eosin (HE) staining

Paraffin sections of mouse brain tissue were deparaffinized, and hydrated with gradient ethanol. Hematoxylin solution (H810910, Macklin) was employed to stain for 10 min and then treated with hydrochloric acid ethanol differentiation solution (C0161s, Beyotime) for 30 s. After full cleaning, 1 % eosin (C0109, Beyotime) was used for staining for 1 min and gradient ethanol was used for dehydration (Dai *et al.*, 2022). The pathological changes of hippocampal CA1 region in mice were observed by DM IL LED microscope (Leica) after sealing with xylene transparent and Neutral Balsam (C0173, Beyotime).

Immunofluorescence

The paraffin sections of mouse brain tissue were first rinsed in PBS and subsequently incubated with 0.3% Triton X-100 at 25°C for 10 min to enhance membrane permeability. 5% bovine serum albumin (BSA, ST023, Beyotime) was added dropwise on the sections and blocked for 1 h. After that, they were incubated overnight with Iba1 primary antibody (PA5-21274, 1:100, Invitrogen, Carlsbad, CA, USA) at 4°C (Ding *et al.*, 2022). The sections were rinsed in PBS for 3 times to remove unbound primary antibody, then incubated with goat anti-rabbit secondary antibody (F-2765,1:500, Invitrogen) at 25°C for 1 h. Once sealed with AntiFade Mounting Medium, the sections were observed using fluorescence microscope.

Nissl staining

Paraffin sections of mouse brain tissue were spread flat in warm water to fully expand and then fished out with slides after the tissue was stretched. The sections were placed in a desiccator and baked at 70°C for 1 h, deparaffinized with xylene for 25 min and rehydrated with gradient alcohol. The liquid on top of the sections was aspirated, and then Nissl staining solution (C0117, Beyotime) was added dropwise onto the surface of the sections and incubated for 10 min (Huang *et al.*, 2023). After sufficient rinsing with tap water, it was immersed in 95% ethanol for 5 min and after dehydration, it was transparent in xylene. The sections were observed by microscope and the area of damaged neurons was analyzed by ImageJ software.

Molecular docking

The molecular docking experiment of Esk and SIRT3 was carried out by Autodock software (The Scripps Research Institute, CA, USA)(Shen *et al.*, 2023). The receptor protein is SIRT3 (PDB ID: 8V5U), whose 3D structure file was downloaded from the PDB database (https://www.rcsb.org/). The protein structure was examined using PyMOL 2.5.4 software (Schrödinger, Inc., NY, USA) in preparation for docking. Perform hydrogenation on proteins and small molecules using AutoDock Tools 1.5.6 (Scripps Research, CA, USA), then run AutoDock Vina 1.2.0 for molecular docking to obtain binding free energy calculations and docking result files.

The positive control selected was the natural ligand NAD^+ cofactor, which co-crystallized with the SIRT3 crystal structure (PDB: 4BV3). Using docking parameters identical to those for Esk, it was re-docked into the SIRT3 active site. Glucose was selected as the negative control, as this molecule failed to stably bind to the SIRT3 active pocket.

Construction and treatment of neuroinflammatory cell model

Mouse microglia BV-2 (SNL-155) was derived from

Wuhan Sunncell Biotechnology (Hubei, China) and grown in BV-2 cell-specific medium (SNLM-155, Wuhan Sunncell Biotechnology). The culture temperature was set to 37°C, containing 5% CO_2 and their medium was replaced every 2 days.

BV-2 cells were exposed to lipopolysaccharide (LPS, 100 ng/mL, L970739, Macklin) for 12 h to induce cell inflammation (Liu *et al.*, 2025b). In the experiment to investigate the impact of Esk on the survival rate of BV-2 cells, cells underwent a 24-hour treatment with Esk (1, 10, 25, 50, 100, 200 μM) for 24 h(Wen *et al.*, 2024). When exploring the inhibitory impact of Esk on cell inflammation, the cells received various Esk concentrations for 24 h, followed by a 12-hour LPS treatment.

SIRT3 short hairpin RNA (shSIRT3) and control plasmid (shNC) were synthesized by Sangon Biotech Co., Ltd. (Shanghai, China). Following the instructions provided with Lipofectamine 3000 (L3000001, Invitrogen), these plasmids were transfected into BV-2 cells. Following 48 h of transfection, the cells were fully lysed with RIPA lysis buffer (P0013B, Beyotime) and SIRT3 protein expression was detected through Western blot (WB) to evaluate the transfection efficiency. In addition, for LPS+Esk+shSIRT3 and LPS+Esk+shNC groups, BV-2 cells underwent transfection with shSIRT3/shNC and then exposed to Esk (50 μM) for 24 h and subsequently subjected to LPS (100 ng/mL) for 12 h(Liu *et al.*, 2025b).

Cell counting kit-8 (CCK-8) assay

BV-2 cells were inoculated into 96-well plates with 1×10^4 cells (100 μL) per well. When the cells were completely adherent (about 12-16 h), the original medium was exchanged for serum-free medium supplemented with Esk at various concentrations and the cells were cultured for another 24h. 10% CCK-8 reagent (HY-K0301, MedChemExpress) was introduced into each well, fully mixed and incubated in dark for 2 h (Zhao *et al.*, 2024). Finally, to calculate cell viability, the OD_{450} value was assessed by microplate reader (1410101, Thermo Fisher Scientific, Waltham, MA, USA).

ELISA

Mouse brain tissues were cut into pieces, carefully ground, fully homogenized and centrifuged and the supernatant was gathered for subsequent analysis. Meanwhile, BV-2 cell culture supernatants were gathered. Mouse Tumor necrosis factor-alpha (TNF-α, ml002095), Interleukin (IL)-1β (ml106733), IL-6 (ml098430) ELISA kits were from Enzyme-linked Biotechnology (Shanghai, China). Different concentrations of the standard and the supernatant were introduced to the ELISA plate, thoroughly mixed and incubated at 37°C for 90 min. Following rinsing with PBS for 3 times, the corresponding antibody working solution was introduced and left to incubate for 1h at 25°C. After that, HRP-labeled Streptavidin was introduced and left to incubate for 20 min. Each well was first added with 50 μL of color reagent A and then added 50 μL of color reagent B, gently shaken and mixed and incubated at 37 °C in dark for 10 min. After that, 50 μL of termination solution was introduced and mixed well to determine OD_{450} value (Xu *et al.*, 2024).

Mitochondrial membrane potential (MMP) assay

The changes of MMP in BV-2 cells and mouse brain tissue were assessed through MMP detection kit (C2006, Beyotime)(Xu *et al.*, 2023b). JC-1 staining solution was mixed with BV-2 cell suspension (1×10^5 cells/mL), the mixture was gently inverted several times to ensure uniform mixing, then incubated for 30 min at 37 °C. After incubation, the cell mixture was centrifuged, the resulting cell pellet was collected and rinsed twice with JC-1 staining buffer. After that, JC-1 stained-cells was detected using BD FACSCalibur™ flow cytometer (BD biosciences, San Jose, CA, USA), with FlowJo software (v10.8, BD biosciences) was employed for analyzing. In addition, the fresh hippocampus of mice was minced, ground and filtered to prepare a single cell suspension and MMP in hippocampus was assessed according to the above method.

Assay of adenosine 5' -triphosphate (ATP) production

ATP production in BV-2 cells and mouse brain tissue was detected by ATP detection kit (S0026, Beyotime)(Ge *et al.*, 2021). BV-2 cells were mixed well with lysis buffer, centrifuged and the supernatant was taken and mixed quickly with ATP detection working solution and chemiluminescence was detected with tecan spark multifunctional microplate reader (Tecan Trading AG, Männedorf, Switzerland). In addition, the fresh hippocampus of mice was minced and the lysate was added to fully homogenize. The supernatant was taken and the ATP production in hippocampus was assessed according to the above method.

Malondialdehyde (MDA) and superoxide dismutase (SOD) assay

The appropriate amount of mouse brain tissue and BV-2 cells were rinsed with PBS to remove residual medium or blood. Next, the SOD sample preparation solution in the SOD Assay kit (S0101S, Beyotime) was introduced, followed by homogenization (for tissues) or lysis (for cells). The mixture was centrifuged and resulting supernatant was gathered as the test sample. The protein level was assessed by BCA protein concentration determination kit (B917925, Macklin). The protein content of each sample was adjusted to 50 μg and the SOD detection buffer was introduced and mixed, then incubated at 37°C for 30 min, with the OD_{450} value was detected (Liu *et al.*, 2021a). In addition, the above-mentioned tissues or cell lysate supernatants were taken to detect MDA levels in mouse brain tissues and BV-2 cells following the MDA Assay kit (S0131 S, Beyotime) instructions.

Reactive oxygen species (ROS) assay

After different treatments, BV-2 cells were rinsed with PBS, mixed well with 2',7'-dichlorofluorescein diacetate (DCFH-DA) probe (10 μM, D6883, Sigma-Aldrich, St. Louis, MO, USA) and left to incubate for 20 min at 25°C in a dark environment (Ge *et al.*, 2021). After centrifugation, the cells were gathered, rinsed with PBS and resuspended in PBS. The ROS levels in the stained BV-2 cells were evaluated using flow cytometer. The fluorescence intensity of DCF was recorded and FlowJo software was employed for analyzing the acquired data.

In addition, the level of mitochondrial ROS (mtROS) was measured following the protocol described by Xu *et al*. (Xu *et al.*, 2023b). The MitoSOX Red indicator (HY-D1055, MedChemExpress) working solution was mixed well with BV-2 cells and left to incubate for 20 min. The staining was analyzed by flow cytometry.

Western blot (WB)

The mouse brain tissue was cut into pieces and the RIPA lysis buffer was introduced to fully grind to extract the protein. Similarly, RIPA lysis buffer served to lyse BV-2 cells after different treatments. After the lysis was completed, the protein content of the obtained samples was calculated using the BCA protein concentration determination kit. Then, the extracted protein was separated through SDS-PAGE electrophoresis, transferred onto a PVDF membrane (Invitrogen) and then blocked with 5 % BSA for 2 h (Ding *et al.*, 2022). The membrane was incubated at 4°C with primary antibodies (Host: Rabbit) Iba1 (PA5-21274, 1:500), CD86 (MA5-32078, 1:2000), inducible nitric oxide synthase (iNOS, PA1-036, 1:500), SIRT3 (PA5-96406, 1:500), p-AMPK (44-1150G, 1:1000), AMPK (PA5-36045, 1:1000), p-mTOR (44-1125G, 1:1000), Brain derived neurotrophic factor (BDNF, PA5-85730, 1:500), synapsin 1 (51-5200, 1:1000), postsynaptic density 95 (PSD95, 51-6900, 1:1000) or mTOR (PA5-34663, 1:3000) overnight. Following three washes of the membrane on the second day, the samples underwent incubation with goat anti-rabbit antibody (31460, 1: 10000) for a period of 2 h. These antibodies were purchased from Invitrogen. The developer solution (HY-K2005, MedChemExpress) was prepared in proportion to the instructions and was evenly dropped onto the membrane and subsequently scanned using a gel imaging system (iBright CL1500, Invitrogen). The gray value was determined after image processing with Image J software and the ratio of gray value to β-actin (PA1-16889, 1:2000, Invitrogen) representing the relative level of each protein.

Statistical analysis

The experiments were conducted a minimum of 3 times each, with the resulting data presented as mean ± standard deviation (Mean±SD). SPSS 26.0 software (IBM SPSS Statistics 26) was employed for statistical analysis. Prism software (Graphpad 9.0) was employed for plotting. Simple comparison between the two groups, when the data obey normality and homogeneity of variance, using t test; when the data obey the normality but the variance is not homogeneous, the corrected t test is utilized; when the data does not obey the normal distribution, the nonparametric Wilonxcon rank sum test is used. Comparison across multiple groups was performed using a one-way analysis of variance and LSD method was utilized for pairwise comparison after the results showed differences. $P<0.05$ denotes a significant difference.

RESULTS

Esk improves cognitive function and hippocampal neuronal injury in POCD mice

Seven days prior to modeling, all mice underwent the Morris water maze test to exclude differences in cognitive function between groups. Mice were then administered Esk or saline via intraperitoneal injection. Water maze tests were conducted on days 3–7 post-modeling, followed by tissue collection. Fig. 1A depicts the experimental timeline. Morris water maze test revealed that the escape latency of POCD mice was approximately 47.7 s, significantly longer than the 24.0 s observed in the control group ($P<0.001$), suggesting that POCD model mice have spatial learning and memory impairments. However, Esk treatment notably improved cognitive function of POCD mice, increasing the time of mice spent in the target quadrant and crossing times, while shortening the escape latency ($P<0.05$), indicating a notable recovery in their cognitive function (Figs. 1B-1D). Tunel staining revealed that the TUNEL-positive rate in hippocampal neurons of POCD mice increased to 79.83%, whereas Esk reduced the TUNEL-positive rate to 55.96% ($P<0.001$), suggesting that it can inhibit neuronal apoptosis (Figs. 1E-1F). HE staining results further revealed significant structural damage in hippocampal CA1 region, characterized by markedly reduced neuronal count and density with disorganized arrangement. Esk administration effectively preserved the normal morphological integrity of hippocampal neurons (Fig. 1G). Nissl staining showed that the number of neurons in the hippocampal CA1 region of POCD mice decreased by 68.92% compared to the control group ($P<0.001$). Following Esk treatment, the neuronal count significantly increased by 31.27% (Figs. 1H-1I). Additionally, expression of BDNF, synapsin 1 and PSD95 was significantly downregulated in the hippocampal tissue of POCD mice ($P<0.001$), whereas Esk treatment significantly increased the expression of these proteins associated with synaptic function (Figs. 1J-1M). Notably, the expression levels of these proteins in mouse brain tissue showed a significant negative correlation with the mice's escape latency period (Fig. S1). The above results collectively indicate that Esk can enhance spatial learning and memory abilities in POCD mice and can also alleviate the damage to hippocampal neurons.

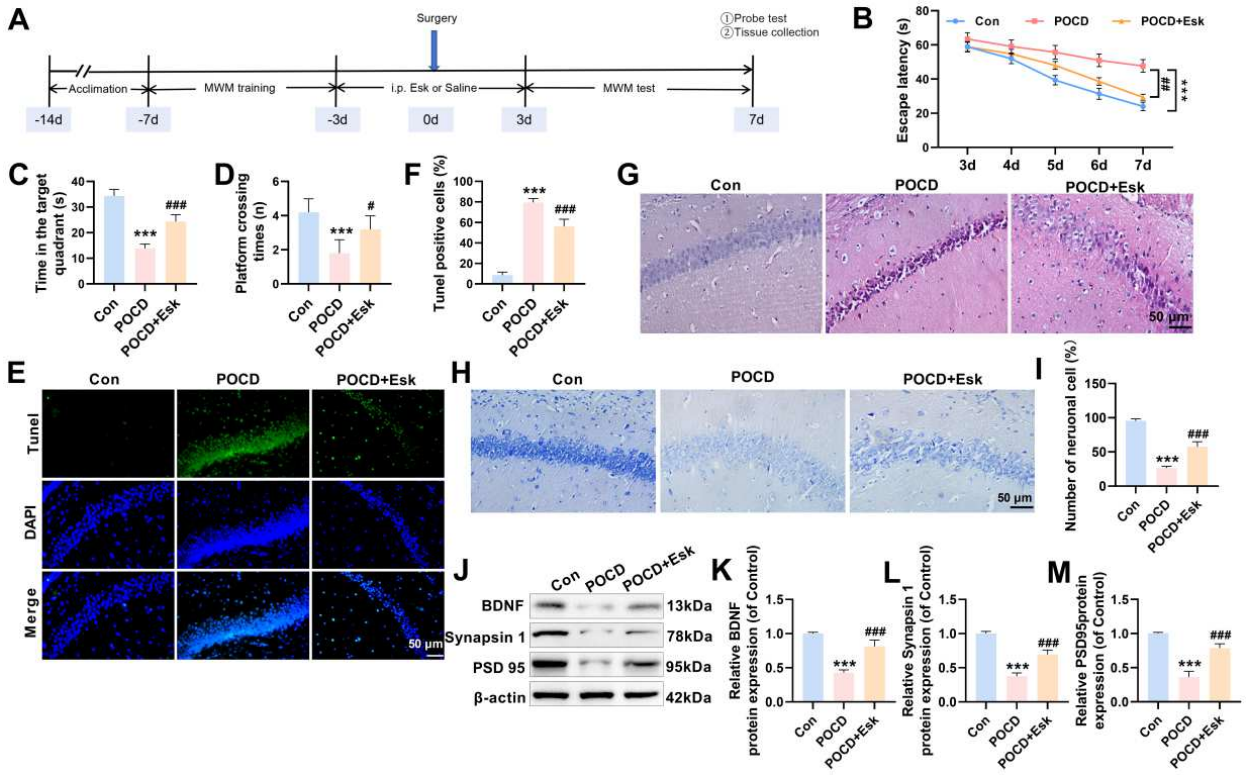

Fig. 1: Esk improves cognitive function and hippocampal neuronal injury in POCD mice
(A) experimental timeline. (B-D) Morris water maze test detected escape latency (B), time spent in target quadrant (C), and hidden platform crossing times (D) of mice. (E-F) TUNEL staining showed that Esk reduced the TUNEL-positive rate of hippocampal neurons in POCD mice (40×, 50 μm). (G) HE staining showed that Esk protected the hippocampal tissue from damage (40×, 50 μm). (H-I) Nissl staining revealed that Esk attenuated neuronal loss in the hippocampal tissue of POCD mice. (40×, 50 μm). (J-M) WB measured BDNF, synapsin 1 and PSD95 levels in POCD mice. n =10 in each group. ***P<0.001 vs Con; #P<0.05, ##P<0.01, ###P<0.001vs POCD.

Esk inhibits M1 polarization of microglia and neuroinflammation of POCD mice

Previous studies have confirmed that microglia M1 polarization and neuroinflammation are crucial components of the pathogenesis of POCD (Hu *et al.*, 2024; Wen *et al.*, 2024). Therefore, we investigated whether Esk improves POCD through modulating microglial polarization and neuroinflammatory responses. Immunofluorescence results revealed that in hippocampal tissue of POCD mice, the fluorescence intensity of Iba1, a microglial-specific marker, was markedly elevated to 62.74%, while Esk treatment markedly reduced Iba1 fluorescence intensity to 17.98% (P<0.001) (Figs. 2A-2B). WB analysis revealed increased protein concentrations of CD86 and iNOS, markers of M1-type microglia in POCD mice and Esk treatment effectively downregulated the expression levels of both (P<0.05) (Figs. 2C-2E). Additionally, ELISA assay kits showed that proinflammatory factor levels (TNF-α, IL-1β and IL-6), were notably higher in the hippocampal tissue of POCD mice. Esk treatment significantly decreased these levels (P<0.05) (Figs. 2F-2H). Thees findings suggest that Esk might exert its effects by inhibiting M1 polarization and neuroinflammatory responses in microglia of POCD mice.

Esk improves mitochondrial dysfunction and oxidative stress levels in POCD mice

Next, we investigated the impacts of Esk on mitochondrial dysfunction and oxidative stress in POCD mice. Mitochondria, as the core site of cellular energy metabolism, their ability to synthesize ATP is an important indicator of functional status (Zhang *et al.*, 2023). ATP assay kit revealed that ATP production in the hippocampal tissue of POCD mice was notably reduced to 44.67 μmol/g protein, whereas Esk treatment significantly increased ATP production to 82.00 μmol/g protein (P<0.01), suggesting that it may enhance mitochondrial energy supply capacity (Fig. 3A). Preserving mitochondrial function relies on the stability of MMP(Xu *et al.*, 2023b). MMP levels were markedly reduced in POCD mice (P<0.01), suggesting abnormal mitochondrial function. Esk treatment effectively increased MMP levels in POCD mice (P<0.05), providing strong support for the improvement of mitochondrial function (Figs. 3B-3C). Notably, pearson correlation analysis revealed a significant negative correlation between escape latency and ATP levels at the individual animal level (Fig. S2).

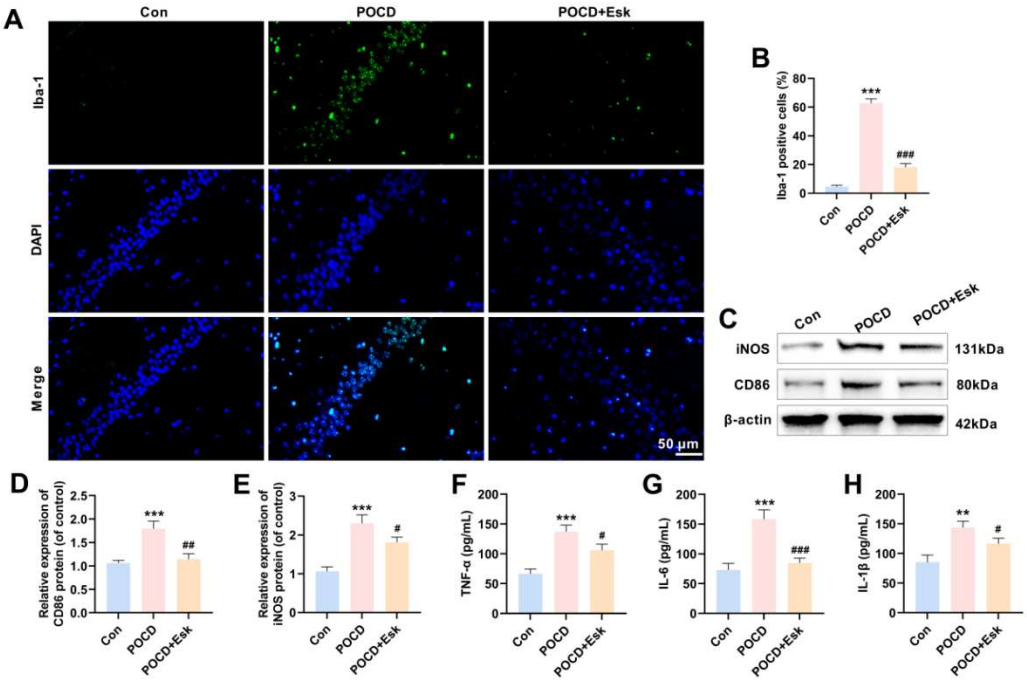

Fig. 2: Esk inhibits M1 polarization and neuroinflammation in microglia of POCD mice
(A-B) Immunofluorescence analysis revealed increased Iba1 fluorescence intensity in the hippocampal tissue of POCD mice, and Esk treatment reduced the fluorescence intensity of Iba1 (40×, 50 μm). (C-E) WB measured elevated CD86 and iNOS levels in POCD mice and Esk treatment reduced the protein levels of both markers. (F-H) ELISA kits showed elevated TNF-α, IL-1β and IL-6 levels in POCD mice, while Esk treatment declined these inflammatory factors levels. n =10 in each group. ***P<0.001 vs Con; #P<0.05, ##P<0.01, ###P<0.001vs POCD.

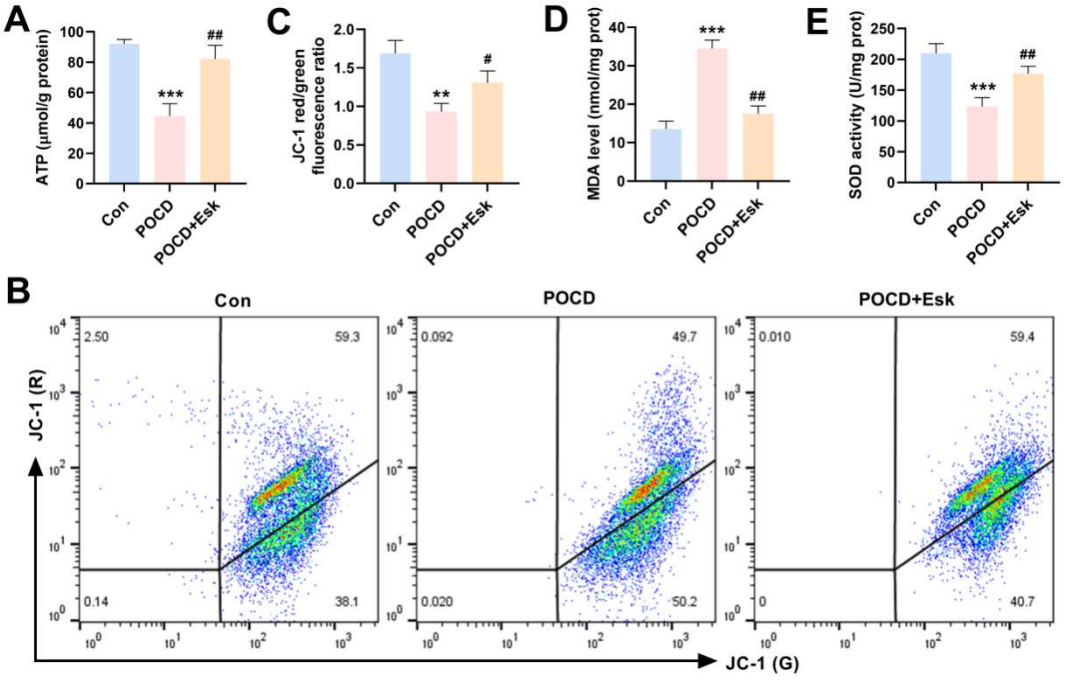

Fig. 3: Esk improves mitochondrial dysfunction and oxidative stress in POCD mice
(A) ATP assay kit showed that Esk treatment increased ATP production. (B-C) MMP assay kit findings indicated that Esk increased the MMP in POCD mice. (D-E) SOD and MDA assay kits measured decreased SOD level and increased MDA level in the brain tissue of POCD mice, but Esk treatment reversed this phenomenon. n =10 in each group. ***P<0.001 vs Con; #P<0.05, ##P<0.01, ###P<0.001vs POCD.

The results of the SOD and MDA assay kits showed that POCD mice had a state of oxidative stress imbalance with decreased SOD levels and increased MDA levels in their brain tissue (P<0.001), while Esk treatment successfully reversed this phenomenon (P<0.01), indicating that it may exert its effects by enhancing antioxidant capacity and alleviating oxidative damage (Figs. 3D-3E). These results indicate that Esk can alleviate mitochondrial dysfunction and oxidative stress damage by improving mitochondrial energy metabolism in hippocampal tissue of POCD mice, stabilizing MMP and regulating oxidative stress balance.

Esk protects neurons by modulating SIRT3/AMPK/mTOR pathway

We assessed the regulatory role of Esk in SIRT3/AMPK/mTOR pathway. In the brain tissue of POCD mice, the relative expression level of SIRT3 decreased to 0.25 and p-AMPK/AMPK level were reduced to 0.45 and p-mTOR/mTOR was elevated to 2.16 (P<0.001), while Esk reversed this phenomenon (P<0.01), suggesting its potential to act by modulating the expression and activity of key molecules in this pathway (Figs. 4A-4D). Further molecular docking results showed that the predicted binding free energy between Esk and SIRT3 is -5.7 kcal/mol (Fig. 4E). The NAD^+ cofactor (positive control) exhibits a high degree of similarity to the native conformation in the SIRT3 crystal structure. In contrast, glucose (negative control) failed to form a stable binding interaction within the SIRT3 active site. This observation provides preliminary molecular-level clues supporting a potential interaction between Esk and SIRT3 and suggests that Esk might exert neuroprotective effects through regulating the SIRT3/AMPK/mTOR pathway.

Esk inhibits M1 polarization in BV-2 cells and neuroinflammation through the SIRT3/AMPK/mTOR pathway

Next, we used LPS-induced BV-2 cells to further investigate the ameliorative impacts of Esk on neuroinflammation. After treating BV-2 cells with Esk for 24 h, the CCK-8 assay indicated that Esk at 1~50 μM did not substantially impact BV-2 cell viability (P>0.05), while Esk concentrations increased to 100 μM and 200 μM, cell viability significantly decreased to 0.68 and 0.65 (P<0.05) (Fig. 5A). In the LPS-induced BV-2 cell inflammation model, pretreatment with 25 and 50 μM Esk significantly improved BV-2 cell viability damage (P<0.05) (Fig. 5B). Among them, 50 μM Esk had the most significant effect on cell viability, so we used this concentration to evaluate the neuroprotective effect of Esk *in vitro*. After LPS treatment, SIRT3 protein and p-AMPK/AMPK level were decreased in BV-2 cells, while p-mTOR/mTOR was raised. Esk treatment reversed these changes induced by LPS (P<0.05) (Figs. 5C-5F). To investigate whether Esk exerts neuroprotective effects by regulating SIRT3/AMPK/mTOR pathway, we transfected shSIRT3 to interfere with SIRT3 expression in BV-2 cells. After shSIRT3 transfection, SIRT3 protein level in BV-2 cells was markedly reduced to 0.44 (P<0.01), confirming the effectiveness of the transfection (Figs. 5G-5H). Silencing SIRT3 significantly reduced the effects of ESK, leading to decreased SIRT3 protein expression levels and p-AMPK/AMPK levels, while p-mTOR/mTOR levels increased (P<0.01) (Figs. 5I-5L). In addition, LPS raised Iba1, CD86 and iNOS proteins levels in BV-2 cells, while Esk treatment reduced these proteins levels (P<0.01), while SIRT3 silencing attenuated the above effects of Esk (Figs. 5M-5P). ELISA kit results also showed a similar trend, with LPS treatment leading to increased IL-1β, IL-6 and TNF-α levels, Esk treatment reducing these inflammatory factors levels (P<0.001), while silencing SIRT3 weakening the effect of Esk (P<0.01) (Figs. 5Q-5S). Moreover, Esk treatment significantly increased the expression of BDNF, synapsin 1 and PSD95 (P<0.001), while silencing SIRT3 reduced the expression of these synapse-associated proteins (P<0.01) (Figs. 5T-5U). The above results indicate that Esk might inhibit BV-2 cell M1 polarization and neuroinflammation caused by LPS via SIRT3/AMPK/mTOR pathway.

Esk improves mitochondrial dysfunction and oxidative stress in BV-2 cells through regulating SIRT3/AMPK/mTOR pathway

Finally, we further investigated whether Esk improves LPS-induced oxidative stress and mitochondrial dysfunction by regulating the SIRT3/AMPK/mTOR pathway. After LPS treatment, ATP production and MMP were decreased (P<0.01), suggesting that LPS treatment caused mitochondrial dysfunction in BV-2 cells. Esk treatment increased ATP production and MMP (P<0.01), but the mitochondrial protective effect of Esk was weakened after SIRT3 silencing (P<0.05) (Fig. 6A-6C). Flow cytometry analysis revealed that LPS treatment increased ROS and mtROS levels in BV-2 cells by 10.41-fold and 2.32-fold (P<0.001), respectively, while Esk addition reduced ROS and mtROS levels by 4.52-fold and 1.74-fold (P<0.001). Silencing SIRT3 weakened the effect of Esk (P<0.01) (Figs. 6D-6G). Additionally, after LPS treatment, SOD level was decreased and MDA level was raised, while Esk treatment reversed this phenomenon (P<0.001). However, silencing SIRT3 reduced the effect of Esk (P<0.01) (Figs. 6H-6I). The findings indicate that Esk could alleviate oxidative stress and mitochondrial dysfunction by modulating SIRT3/AMPK/mTOR pathway.

DISCUSSION

The exact pathogenesis of POCD is still unknown and there are currently no specific drug treatments available. This situation highlights the urgent need to develop new treatment strategies (Kong *et al.*, 2022). Previous researches have shown that mitochondrial dysfunction, neuroinflammation and oxidative stress have a significant impact on the occurrence of POCD (Yang *et al.*, 2022).

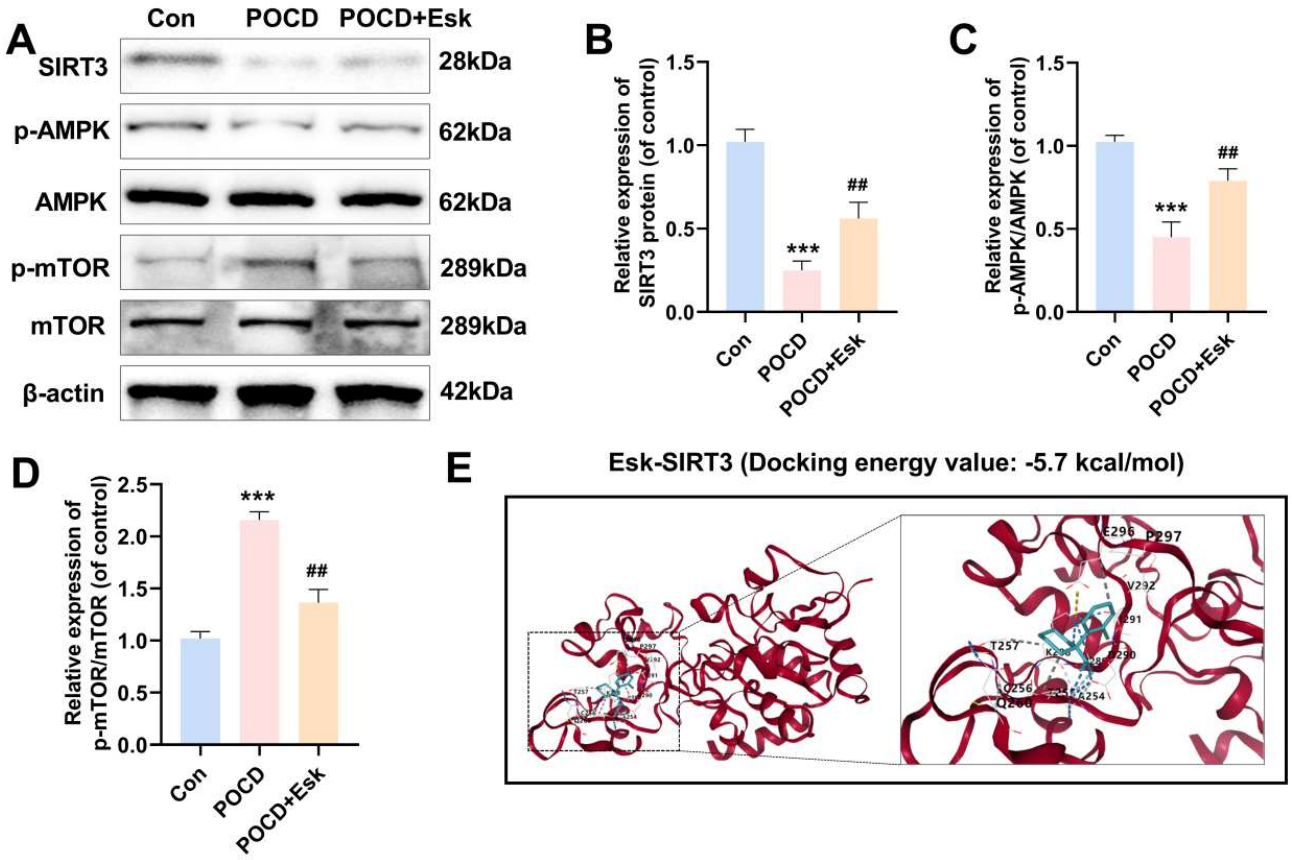

Fig. 4: Esk exerts neuroprotective properties via regulating SIRT3/AMPK/mTOR pathway
(A-D) WB analysis indicated reduced SIRT3 and p-AMPK/AMPK levels and increased p-mTOR/mTOR level in the brain tissue of POCD mice, while Esk treatment reversed this phenomenon. (E) molecular docking results showed that Esk and SIRT3 have good binding activity. n =10 in each group. ***P<0.001 vs Con; #P<0.05, ##P<0.01, ###P<0.001vs POCD.

We adopted the research methods of previous studies and constructed a POCD aged mouse model using a modified abdominal exploration laparotomy, compared to young mice, aged mice exhibit increased blood-brain barrier permeability and higher baseline inflammation levels, making them more susceptible to postoperative glial cell dysregulation and cognitive decline. This aligns closely with the pathological characteristics underlying the high incidence of POCD in elderly clinical patients (Li *et al.*, 2025). Microglia are characterized by their multi-synaptic and plastic properties and are responsible for monitoring the brain and initiating an initial response to neuroinflammation caused by surgical trauma or pathogens (Xu *et al.*, 2023a; Shi and Yong, 2025). Numerous investigations have shown that excessive activation of microglia could be observed in POCD mice (Han *et al.*, 2022; Kong *et al.*, 2024). The M1/M2 phenotype balance of microglia is key to maintaining central immune homeostasis. M1-type microglia release proinflammatory factors that can directly damage neuronal synapses, while M2-type microglia release anti-inflammatory factors (Liu *et al.*, 2021b; Guo *et al.*, 2022). Pro-inflammatory mediators such as LPS can induce microglia to differentiate into the M1 phenotype, resulting in morphological abnormalities, synaptic abnormalities and mitochondrial abnormalities (Liu *et al.*, 2025b). Therefore, we used LPS-induced microglia as an *in vitro* model for studying POCD. In this study, mice in the POCD group exhibited spatial learning and memory impairments, neuroinflammation and neuronal apoptosis, with high expression of the microglia activation marker Iba1. In the LPS group, BV-2 cells exhibited M1 polarization and reduced cell viability, implying that the POCD model was established successfully.

The role of Esk in neuroprotection has attracted widespread attention in recent years. In a mouse model of cerebral hemorrhage, 20 mg/kg of Esk reduced neurological damage, promoted nerve repair, improved cognitive function and had no adverse effects on the liver and kidneys of mice (Jiang *et al.*, 2024). It is worth noting that the effective dose of Esk used in this study (5 mg/kg) differs from that in the aforementioned research. This discrepancy arises from variations in disease pathology, experimental animal conditions and intervention targets. In this study, the 5 mg/kg dose was selected for aged POCD mice to avoid potential toxicity associated with higher dosages.

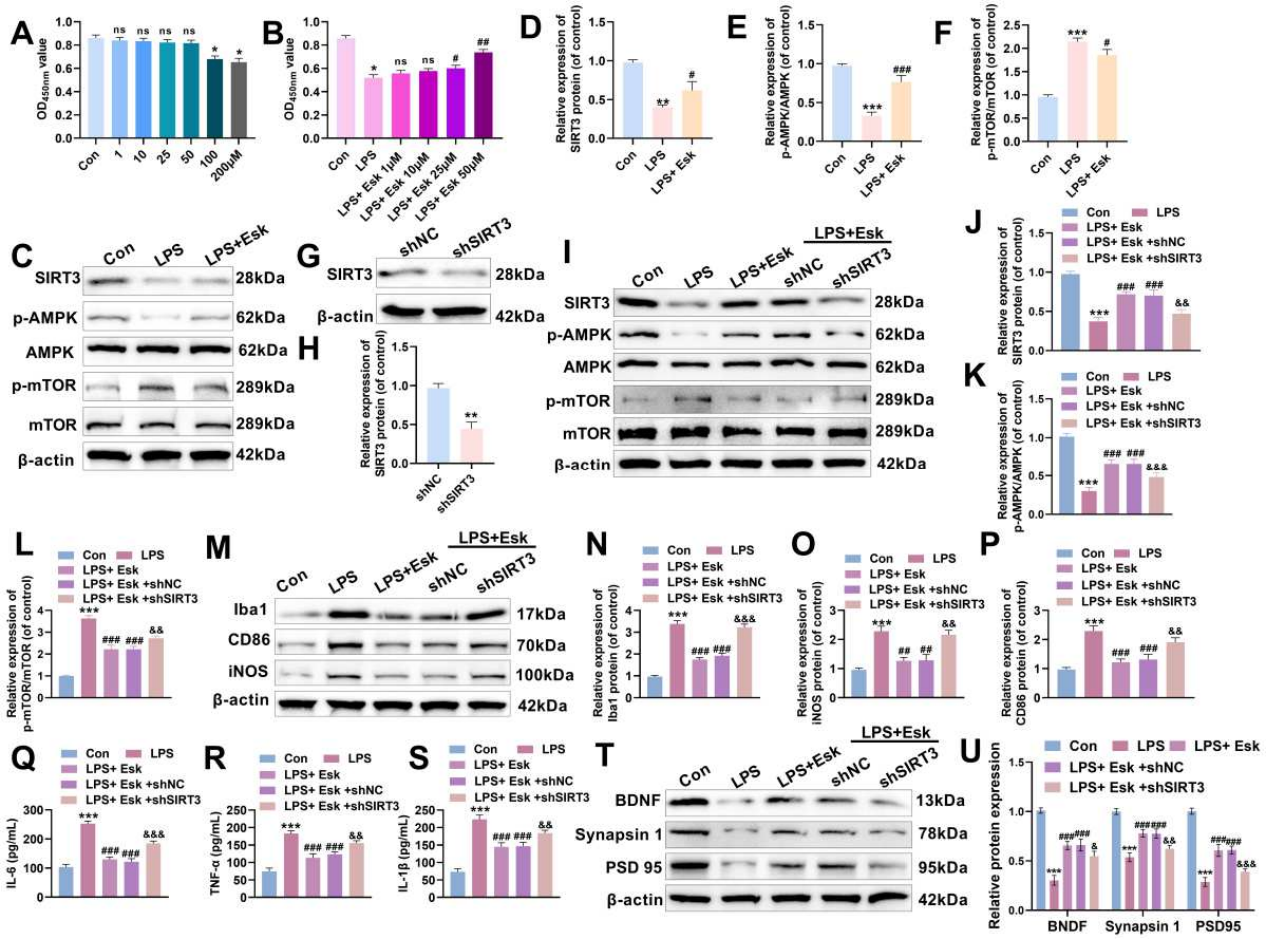

Fig. 5: Esk inhibits BV-2 cell M1 polarization and neuroinflammation through SIRT3/AMPK/mTOR pathway
(A) CCK-8 assay detected the viability of BV-2 cells exposed to Esk (1, 10, 25, 50, 100, 200 μM) for 24 h. (B) CCK-8 assay confirmed that LPS caused a decrease in BV-2 cell viability, while treatment with 25 and 50 μM Esk increased BV-2 cell viability. (C-F) WB measured that LPS treatment reduced SIRT3 and p-AMPK/AMPK levels and increased p-mTOR/mTOR levels in BV-2 cells, while Esk treatment reversed the effects of LPS treatment. (G-H) WB revealed that SIRT3 was downregulated in BV-2 cells following shSIRT3 transfection. (I-L) WB detection of SIRT3/AMPK/mTOR pathway-related protein expression in BV-2 cells following SIRT3 silencing. (M-P) WB results indicated that LPS raised Iba1, CD86 and iNOS levels, while Esk treatment reduced these proteins levels, silencing SIRT3 weakened the effect of Esk. (Q-S) ELISA assay kits detected that LPS caused elevated IL-1β, IL-6 and TNF-α levels, Esk treatment reduced these inflammatory factors levels, and silencing SIRT3 attenuated the effect of Esk. (T-U) WB measured BDNF, synapsin 1 and PSD95 levels in BV-2 cells following SIRT3 silencing. n =5 in each group. **P*<0.05, ***P*<0.01, ****P*<0.001 vs Con; #*P*<0.05, ##*P*<0.01, ###*P*<0.001vs LPS; &&*P*<0.01, &&&*P*<0.001 vs LPS+Esk+shNC.

In this study, we found that Esk (5 mg/kg) effectively improved memory abilities of POCD mice. Cognitive impairment in POCD is closely related to the disruption of hippocampal neural circuits (Wu *et al.*, 2022; Wu *et al.*, 2024). Pathological staining showed that Esk alleviated pathological damage to hippocampal tissue and neuronal apoptosis and inhibited the activation of microglia. Therefore, we propose that the enhancement of spatial memory in mice by Esk may be related to its protection of hippocampal neurons. In the LPS-induced BV-2 cell inflammation model, Esk (50 μM) pretreatment increased cell viability, declined inflammatory factors levels and downregulated M1 polarization markers (CD86 and iNOS). In a cerebral ischemia/reperfusion injury rat model, Gao *et al*. also made similar findings, showing that Esk inhibited microglia M1 polarization and stimulate M2 polarization (Gao *et al.*, 2025). Compared to previous studies, the key value of this research lies in validating Esk's anti-inflammatory effects within the POCD-associated inflammatory microenvironment. Furthermore, through *in vitro* cellular models, factors such as peripheral inflammation and metabolic disorders induced by surgical trauma *in-vivo* were excluded. This suggests that Esk has the ability to suppress neuroinflammation and may be a potential drug for treating POCD.

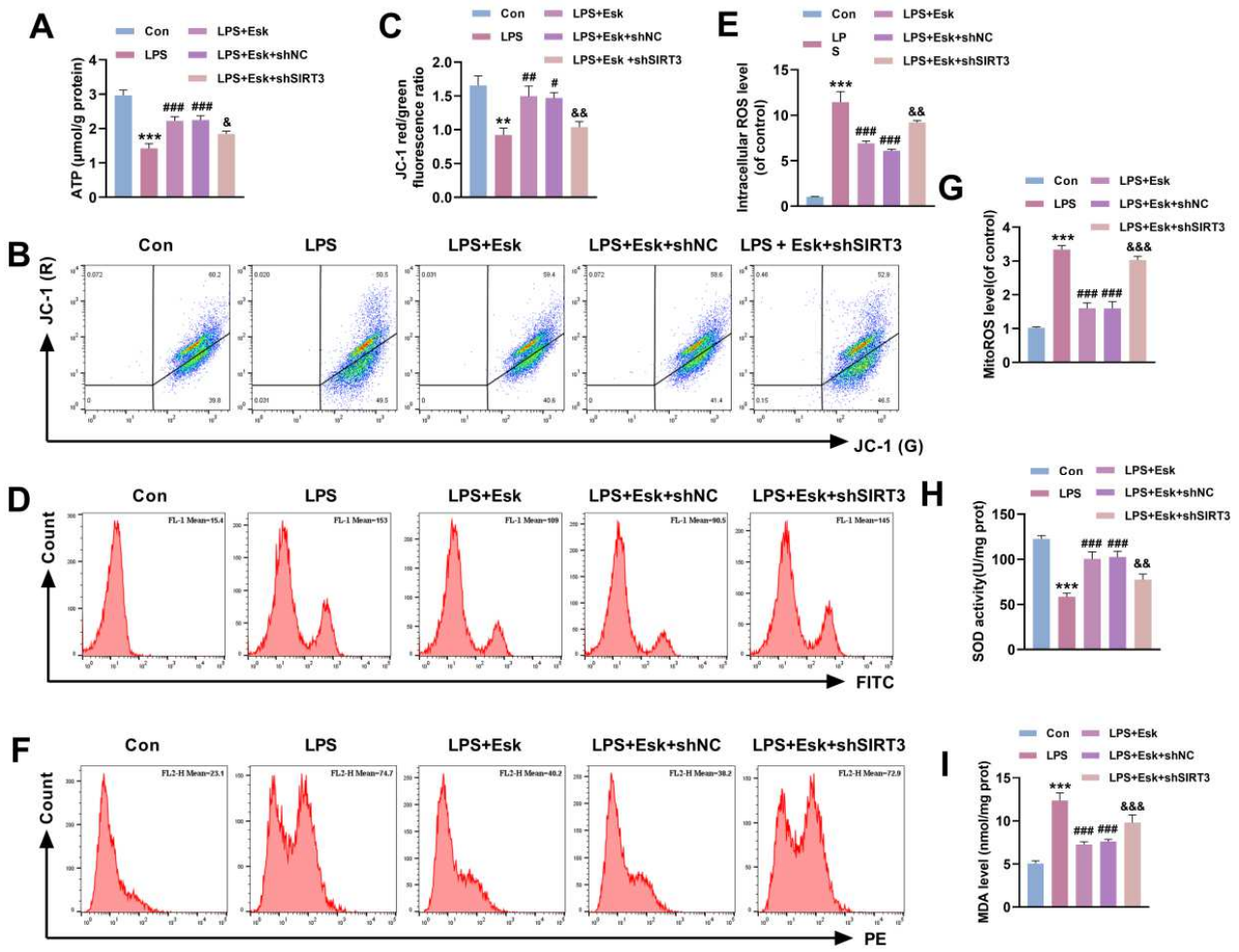

Fig. 6: Esk improves mitochondrial dysfunction and oxidative stress through regulating SIRT3/AMPK/mTOR pathway (A) ATP assay kit revealed that LPS declined ATP production in BV-2 cells, while Esk treatment increased ATP production, but silencing SIRT3 weakened this effect. (B-C) MMP assay demonstrated that LPS decreased MMP level, Esk treatment increased MMP in BV-2 cells and SIRT3 silencing reduced the effect of Esk. (D-E) flow cytometry revealed that LPS increased ROS levels, Esk treatment reduced ROS levels in BV-2 cells and SIRT3 silencing weakened this effect. (F-G) flow cytometry showed that LPS treatment increased mtROS levels in BV-2 cells, while Esk treatment decreased mtROS levels and SIRT3 silencing weakened the effect of Esk. (H-I) SOD and MDA kits showed that LPS treatment decreased SOD levels and increased MDA levels, but Esk treatment reversed this phenomenon and SIRT3 silencing decreased the effect of Esk. n =5 in each group. ***P*<0.01, ****P*<0.001 vs Con; #*P*<0.05, ##*P*<0.01, ###*P*<0.001vs LPS; &*P*<0.05, &&*P*<0.01, &&&*P*<0.001 vs LPS+Esk+shNC.

Mitochondria are the core of cellular energy metabolism and energy metabolism failure caused by mitochondrial dysfunction is an important trigger for neuronal apoptosis(Moradi Vastegani *et al.*, 2023; Lan *et al.*, 2024). Surgical trauma-induced mitochondrial dysfunction can exacerbate POCD through multiple pathways. For example, insufficient ATP production leads to neuronal dysfunction; the excessive production of mtROS causes oxidative damage to lipids, proteins and DNA(Yang *et al.*, 2022; Xu *et al.*, 2023b; Bonfante *et al.*, 2024; Ying *et al.*, 2024). In this study, Esk improved mitochondrial function in POCD mice by increasing ATP production and MMP, which provides energy for neuronal survival. It also increased SOD activity and reduced MDA level, implying that it can inhibit oxidative stress. Furthermore, Esk reduced ROS and mtROS levels, confirming its ability to improve oxidative stress and mitochondrial dysfunction at the cellular level.

SIRT3 protein is commonly expressed in mitochondria-rich tissues including the heart, blood vessels, kidneys, brain and liver, serves a crucial role in regulating mitochondrial function (Ji *et al.*, 2022; Ning *et al.*, 2024). Research indicates that SIRT3 is downregulated in POCD mouse models, while overexpression of SIRT3 improves cognitive function in mice, enhances synaptic plasticity and inhibits oxidative stress and neuroinflammation (Liu *et al.*, 2021a). There is substantial evidence indicating that

SIRT3 regulates the AMPK/mTOR pathway (Xin and Lu, 2020; Wang *et al.*, 2024; Wang *et al.*, 2025a). Additionally, SIRT3 also mediates autophagy by regulating AMPK/mTOR pathway, thus suppressing neuroinflammation and reducing cognitive dysfunction in POCD mice (Li *et al.*, 2022). The SIRT3/AMPK/mTOR pathway is a core regulatory network for cellular responses to metabolic stress and its imbalance is closely linked with neuronal damage in diseases like cerebral ischemia-reperfusion and subarachnoid hemorrhage (Liu *et al.*, 2020; Wang *et al.*, 2025b). We found that SIRT3 protein and AMPK phosphorylation levels were notably reduced in POCD mice and LPS-treated BV-2 cells, while mTOR phosphorylation level was increased. Esk treatment reversed the abnormal expression of SIRT3/AMPK/mTOR pathway-related proteins, suggesting that Esk can regulate this pathway and molecular docking confirmed that Esk has strong binding activity with SIRT3. Moreover, silencing SIRT3 weakened the inhibitory effects of Esk on M1 polarization and neuroinflammation and exacerbated mitochondrial dysfunction and oxidative stress. These results confirm that Esk may inhibit the progression of POCD via regulating SIRT3/AMPK/mTOR pathway to suppress M1 polarization of microglia, neuroinflammation, mitochondrial dysfunction and oxidative stress. We must acknowledge that this study employed only a single dose of Esk and did not conduct dose-response investigations, making it difficult to determine the optimal therapeutic window. In future experiments, we will conduct gradient concentration studies to further determine the safe dosage range and optimal therapeutic window for Esk and investigate its potential side effects in elderly patients. Although we cannot entirely rule out the possibility that Esk indirectly influences the findings of this study through its complex multi-target properties, the evidence presented—including SIRT3 function-dependent experiments, consistent activation of molecular pathways across models and the dissociation of its cognitive protective effects from the state of light anesthesia—strongly supports the activation of the SIRT3/AMPK/mTOR pathway as the core mechanism by which Esk improves POCD in aged mice. Moreover, one of the most significant translational implications of this study is our discovery that the neuroprotective effects of Esk depend on SIRT3 activation. This mechanistic finding provides robust scientific rationale for the future development of novel drugs selectively targeting the SIRT3 pathway, such as SIRT3-specific agonists.

CONCLUSION

In summary, Esk can inhibit microglia M1 polarization and neuroinflammation via regulating SIRT3/AMPK/mTOR pathway, improve mitochondrial dysfunction, alleviate hippocampal neuronal damage and thereby improve POCD in aged mice. This study clarified the potential mechanism by which Esk hinders POCD progression, expanded the pharmacological effects of Esk and provided potential drugs and therapeutic targets for POCD treatment. Nevertheless, the current study still has some limitations and subsequent studies can further verify the efficacy of Esk in different POCD models.

Acknowledgment
None

Authors' contributions
Yunfei Wang and Tao Cui: Conducted and designed the research, carried out experiments and analyzed findings. Edited and refined the manuscript with a focus on critical intellectual contributions; Jiafang Wang and Li Zhang: Participated in collecting, assessing and interpreting the data. Made significant contributions to data interpretation and manuscript preparation; Lu Zou and Zhe Ding: Provided substantial intellectual input during the drafting and revision of the manuscript.The final version of the manuscript has been reviewed and approved by all authors.

Funding
The National Natural Science Foundation of China (NO. 82401721)

Data availability statement
The datasets generated during and/or analysed during the current study are available from the corresponding author on reasonable request.

Ethical approval
This study was approved by the Department of Anesthesiology, Wuhan No.1 Hospital Ethics Committee [(2024)33]

Conflicts of interest
The authors affirm that they have no conflicts of interest.

Consent to participate
We secured a signed informed consent form from every participant.

Supplementary data
https://www.pjps.pk/uploads/2026/03/SUP1772954605.pdf

REFERENCES

Anand N, Gupta R, Mishra S P and Mishra M (2024). Postoperative cognitive dysfunction: A review. *Asian J Anesthesiol*. **62**(1): 1-11.

Bahji A, Zarate C A and Vazquez G H (2022). Efficacy and safety of racemic ketamine and esketamine for depression: A systematic review and meta-analysis. *Expert Opin Drug Saf*. **21**(6): 853-866.

Bhushan S, Li Y, Huang X, Cheng H, Gao K and Xiao Z (2021). Progress of research in postoperative cognitive

dysfunction in cardiac surgery patients: A review article. *Int J Surg*. **95**: 106163.

Bonfante S, Netto M B, de Oliveira Junior A N, Mathias K, Machado R S, Joaquim L, Cidreira T, da Silva M G, Daros G C, Danielski L G, Gava F, da Silva Lemos I, Matiola R T, Córneo E, Prophiro J S, de Bitencourt R M, Catalão C H R, da Silva Generoso J, Streck E L, Dal-Pizzol F, Barichello T and Petronilho F (2024). Oxidative stress and mitochondrial dysfunction contributes to postoperative cognitive dysfunction in elderly rats dependent on NLRP3 activation. *Metab Brain Dis*. **40**(1): 1.

Dai S, Wei J, Zhang H, Luo P, Yang Y, Jiang X, Fei Z, Liang W, Jiang J and Li X (2022). Intermittent fasting reduces neuroinflammation in intracerebral hemorrhage through the Sirt3/Nrf2/HO-1 pathway. *J Neuroinflammation*. **19**(1): 122.

Ding R, Li H, Liu Y, Ou W, Zhang X, Chai H, Huang X, Yang W and Wang Q (2022). Activating cGAS-STING axis contributes to neuroinflammation in CVST mouse model and induces inflammasome activation and microglia pyroptosis. *J Neuroinflammation*. **19**(1): 137.

Feeney A and Papakostas G I (2023). Pharmacotherapy: Ketamine and Esketamine. *Psychiatr Clin North Am*. **46**(2): 277-290.

Gao Y, Li L, Zhao F, Cheng Y, Jin M and Xue F S (2025). Esketamine at a clinical dose attenuates cerebral ischemia/reperfusion injury by inhibiting akt signaling pathway to facilitate microglia M2 polarization and autophagy. *Drug Des Devel Ther*. **19**: 369-387.

Ge X, Zuo Y, Xie J, Li X, Li Y, Thirupathi A, Yu P, Gao G, Zhou C, Chang Y and Shi Z (2021). A new mechanism of POCD caused by sevoflurane in mice: Cognitive impairment induced by cross-dysfunction of iron and glucose metabolism. *Aging (Albany NY)*. **13**(18): 22375-22389.

Guo S, Wang H and Yin Y (2022). Microglia polarization from M1 to M2 in neurodegenerative diseases. *Front Aging Neurosci*. **14**: 815347.

Guo Y, Jia X, Cui Y, Song Y, Wang S, Geng Y, Li R, Gao W and Fu D (2021). Sirt3-mediated mitophagy regulates AGEs-induced BMSCs senescence and senile osteoporosis. *Redox Biol*. **41**: 101915.

Han C, Ji H, Guo Y, Fei Y, Wang C, Yuan Y, Ruan Z and Ma T (2023). Effect of subanesthetic dose of esketamine on perioperative neurocognitive disorders in elderly undergoing gastrointestinal surgery: A randomized controlled trial. *Drug Des Devel Ther*. **17**: 863-873.

Han X, Cheng X, Xu J, Liu Y, Zhou J, Jiang L, Gu X and Xia T (2022). Activation of TREM2 attenuates neuroinflammation via PI3K/Akt signaling pathway to improve postoperative cognitive dysfunction in mice. *Neuropharmacology*. **219**: 109231.

Hu H, Cao B, Huang D, Lin Y, Zhou B, Ying J, Huang L and Zhang L (2024). Withaferin a modulation of microglia autophagy mitigates neuroinflammation and enhances cognitive function in POCD. *Sci Rep*. **14**(1): 26112.

Huang X, Ye C, Zhao X, Tong Y, Lin W, Huang Q, Zheng Y, Wang J, Zhang A and Mo Y (2023). TRIM45 aggravates microglia pyroptosis via Atg5/NLRP3 axis in septic encephalopathy. *J Neuroinflammation*. **20**(1): 284.

Ji Z, Liu G H and Qu J (2022). Mitochondrial sirtuins, metabolism, and aging. *J Genet Genomics*. **49**(4): 287-298.

Jiang Y, Zeng X, Dai H, Luo S and Zhang X (2024). Polygonatum sibiricum polysaccharide regulation of gut microbiota: A viable approach to alleviate cognitive impairment. *Int J Biol Macromol*. **277**(Pt 3): 134494.

Jonkman K, Duma A, Olofsen E, Henthorn T, van Velzen M, Mooren R, Siebers L, van den Beukel J, Aarts L, Niesters M and Dahan A (2017). Pharmacokinetics and bioavailability of inhaled esketamine in healthy volunteers. *Anesthesiology*. **127**(4): 675-683.

Kong H, Xu L M and Wang D X (2022). Perioperative neurocognitive disorders: A narrative review focusing on diagnosis, prevention, and treatment. *CNS Neurosci Ther*. **28**(8): 1147-1167.

Kong X, Lyu W, Lin X, Lin C, Feng H, Xu L, Shan K, Wei P and Li J (2024). Itaconate alleviates anesthesia/surgery-induced cognitive impairment by activating a Nrf2-dependent anti-neuroinflammation and neurogenesis via gut-brain axis. *J Neuroinflammation*. **21**(1): 104.

Lan X, Wang Q, Liu Y, You Q, Wei W, Zhu C, Hai D, Cai Z, Yu J, Zhang J and Liu N (2024). Isoliquiritigenin alleviates cerebral ischemia-reperfusion injury by reducing oxidative stress and ameliorating mitochondrial dysfunction via activating the Nrf2 pathway. *Redox Biol*. **77**: 103406.

Li H, Hu W, Wu Z, Tian B, Ren Y and Zou X (2024). Esketamine improves cognitive function in sepsis-associated encephalopathy by inhibiting microglia-mediated neuroinflammation. *Eur J Pharmacol*. **983**: 177014.

Li S, Zhou Y, Hu H, Wang X, Xu J, Bai C, Yuan J and Zhang D (2022). SIRT3 enhances the protective role of propofol in postoperative cognitive dysfunction via activating autophagy mediated by AMPK/mTOR pathway. *Front Biosci (Landmark Ed)*. **27**(11): 303.

Li X, Li X, Zhang Q, Li Y, Zhou Y, Zhou J and Duan X (2025). Prostaglandin endoperoxide synthase 2 regulates neuroinflammation to mediate postoperative cognitive dysfunction in mice. *Sci Rep*. **15**(1): 17355.

Liu F, Wu X, Wang Z, Li A, Luo Y and Cao J (2025a). Mitochondrial dysfunction in postoperative cognitive dysfunction: From preclinical mechanisms to multimodal diagnostics and precision intervention. *Ageing Res Rev*. **111**: 102845.

Liu J, Wang Y, Sun H, Lei D, Liu J, Fei Y, Wang C and Han C (2025b). Resveratrol ameliorates postoperative cognitive dysfunction in aged mice by regulating

microglial polarization through CX3CL1/CX3CR1 signaling axis. *Neurosci Lett*. **847**: 138089.

Liu Q, Sun Y M, Huang H, Chen C, Wan J, Ma L H, Sun Y Y, Miao H H and Wu Y Q (2021a). Sirtuin 3 protects against anesthesia/surgery-induced cognitive decline in aged mice by suppressing hippocampal neuroinflammation. *J Neuroinflammation*. **18**(1): 41.

Liu S, Su Y, Sun B, Hao R, Pan S, Gao X, Dong X, Ismail A M and Han B (2020). Luteolin protects against CIRI, potentially via regulation of the SIRT3/AMPK/mTOR signaling pathway. *Neurochem Res*. **45**(10): 2499-2515.

Liu X, Zhang M, Liu H, Zhu R, He H, Zhou Y, Zhang Y, Li C, Liang D, Zeng Q and Huang G (2021b). Bone marrow mesenchymal stem cell-derived exosomes attenuate cerebral ischemia-reperfusion injury-induced neuroinflammation and pyroptosis by modulating microglia M1/M2 phenotypes. *Exp Neurol*. **341**: 113700.

Ma X, Xue S, Ma H, Saeed S, Zhang Y, Meng Y, Chen H, Yu H, Wang H, Hu S and Cai M (2025). Esketamine alleviates LPS-induced depression-like behavior by activating Nrf2-mediated anti-inflammatory response in adolescent mice. *Neuroscience*. **567**: 294-307.

Moradi Vastegani S, Nasrolahi A, Ghaderi S, Belali R, Rashno M, Farzaneh M and Khoshnam S E (2023). Mitochondrial dysfunction and parkinson's disease: Pathogenesis and therapeutic strategies. *Neurochem Res*. **48**(8): 2285-2308.

Neskovic N, Budrovac D, Kristek G, Kovacic B and Skiljic S (2025). Postoperative cognitive dysfunction: Review of pathophysiology, diagnostics and preventive strategies. *J Perioper Pract*. **35**(1-2): 47-56.

Ning Y, Dou X, Wang Z, Shi K, Wang Z, Ding C, Sang X, Zhong X, Shao M, Han X and Cao G (2024). SIRT3: A potential therapeutic target for liver fibrosis. *Pharmacol Ther*. **257**: 108639.

Pavlidi P, Megalokonomou A, Sofron A, Kokras N and Dalla C (2021). Pharmacology of ketamine and esketamine as rapid-acting antidepressants. *Psychiatriki*. **32**(Supplement I): 55-63.

Peng W, Lu W, Jiang X, Xiong C, Chai H, Cai L and Lan Z (2023). Current progress on neuroinflammation-mediated postoperative cognitive dysfunction: An update. *Curr Mol Med*. **23**(10): 1077-1086.

Ravizza T, Scheper M, Di Sapia R, Gorter J, Aronica E and Vezzani A (2024). mTOR and neuroinflammation in epilepsy: implications for disease progression and treatment. *Nat Rev Neurosci*. **25**(5): 334-350.

Rump K and Adamzik M (2022). Epigenetic mechanisms of postoperative cognitive impairment induced by anesthesia and neuroinflammation. *Cells*. **11**(19): 2954.

Shen X, Shi H, Chen X, Han J, Liu H, Yang J, Shi Y and Ma J (2023). Esculetin alleviates inflammation, oxidative stress and apoptosis in intestinal ischemia/reperfusion injury via targeting SIRT3/AMPK/mTOR signaling and regulating autophagy. *J Inflamm Res*. **16**: 3655-3667.

Shi F D and Yong V W (2025). Neuroinflammation across neurological diseases. *Science*. **388**(6753): eadx0043.

Shoib S, Kotra M, Javed S, Nguyen V S and Malathesh B C (2022). Esketamine-A quick-acting novel antidepressant without the disadvantages of ketamine. *Horm Mol Biol Clin Investig*. **43**(4): 505-511.

Tang Y, Liu Y, Zhou H, Lu H, Zhang Y, Hua J and Liao X (2023). Esketamine is neuroprotective against traumatic brain injury through its modulation of autophagy and oxidative stress via AMPK/mTOR-dependent TFEB nuclear translocation. *Exp Neurol*. **366**: 114436.

Trefts E and Shaw RJ (2021). AMPK: restoring metabolic homeostasis over space and time. *Mol Cell*. **81**(18): 3677-3690.

Varpaei H A, Farhadi K, Mohammadi M, Khafaee Pour Khamseh A and Mokhtari T (2024). Postoperative cognitive dysfunction: A concept analysis. *Aging Clin Exp Res*. **36**(1): 133.

Vekhova KA, Namiot ED, Jonsson J and Schioth HB (2025). Ketamine and esketamine in clinical trials: FDA-approved and emerging indications, trial trends with putative mechanistic explanations. *Clin Pharmacol Ther*. **117**(2): 374-386.

Wang J, Yang J H, Xiong D and Chen L (2025a). Activation of SIRT3/AMPK/mTOR-mediated autophagy promotes quercetin-induced ferroptosis in oral squamous cell carcinoma. *Hum Exp Toxicol*. **44**: 9603271251323753.

Wang W, Li Y, Li Y, Zhao Y M, Ye J B and Qian T (2025b). Tetrandrine mediates autophagy via sirtuin 3/adenosine 5-monophosphate-activated protein kinase/mammalian target of rapamycin signal pathway to attenuate early brain injury after subarachnoid hemorrhage. *Neuroreport*. **36**(10): 514-523.

Wang X H, Ning Z H, Xie Z, Ou Y, Yang J Y, Liu Y X, Huang H, Tang H F, Jiang Z S and Hu H J (2024). SIRT3/AMPK signaling pathway regulates lipid metabolism and improves vulnerability to atrial fibrillation in dahl salt-sensitive rats. *Am J Hypertens*. **37**(11): 901-908.

Wang Y, Cai Z, Zhan G, Li X, Li S, Wang X, Li S and Luo A (2023). Caffeic acid phenethyl ester suppresses oxidative stress and regulates M1/M2 microglia polarization via Sirt6/Nrf2 pathway to mitigate cognitive impairment in aged mice following anesthesia and surgery. *Antioxidants (Basel)*. **12**(3): 714.

Wen Y, Xu J, Shen J, Tang Z, Li S, Zhang Q, Li J and Sun J (2024). Esketamine prevents postoperative emotional and cognitive dysfunction by suppressing microglial M1 polarization and regulating the BDNF-TrkB pathway in ageing rats with preoperative sleep disturbance. *Mol Neurobiol*. **61**(8): 5680-5698.

Wu W F, Chen C, Lin J T, Jiao X H, Dong W, Wan J, Liu Q, Qiu Y K, Sun A, Liu Y Q, Jin C H, Huang H, Zheng H, Zhou C H and Wu Y Q (2024). Impaired synaptic plasticity and decreased glutamatergic neuron excitability induced by SIRT1/BDNF downregulation in the hippocampal CA1 region are involved in

postoperative cognitive dysfunction. *Cell Mol Biol Lett*. **29**(1): 79.

Wu Z, Tan J, Lin L, Zhang W and Yuan W (2022). microRNA-140-3p protects hippocampal neuron against pyroptosis to attenuate sevoflurane inhalation-induced post-operative cognitive dysfunction in rats via activation of HTR2A/ERK/Nrf2 axis by targeting DNMT1. *Cell Death Discov*. **8**(1): 290.

Xin T and Lu C (2020). SirT3 activates AMPK-related mitochondrial biogenesis and ameliorates sepsis-induced myocardial injury. *Aging (Albany NY)*. **12**(16): 16224-16237.

Xu F, Han L, Wang Y, Deng D, Ding Y, Zhao S, Zhang Q, Ma L and Chen X (2023a). Prolonged anesthesia induces neuroinflammation and complement-mediated microglial synaptic elimination involved in neurocognitive dysfunction and anxiety-like behaviors. *BMC Med*. **21**(1): 7.

Xu H J, Li X P and Han L Y (2024). Role and mechanism of esketamine in improving postoperative cognitive dysfunction in aged mice through the TLR4/MyD88/p38 MAPK pathway. *Kaohsiung J Med Sci*. **40**(1): 63-73.

Xu X, Gao W, Li L, Hao J, Yang B, Wang T, Li L, Bai X, Li F, Ren H, Zhang M, Zhang L, Wang J, Wang D, Zhang J and Jiao L (2021). Annexin A1 protects against cerebral ischemia-reperfusion injury by modulating microglia/macrophage polarization via FPR2/ALX-dependent AMPK-mTOR pathway. *J Neuroinflammation*. **18**(1): 119.

Xu X, Zhou B, Liu J, Ma Q, Zhang T and Wu X (2023b). Ru360 alleviates postoperative cognitive dysfunction in aged mice by inhibiting MCU-mediated mitochondrial dysfunction. *Neuropsychiatr Dis Treat*. **19**: 1531-1542.

Yang Y, Liu Y, Zhu J, Song S, Huang Y, Zhang W, Sun Y, Hao J, Yang X, Gao Q, Ma Z, Zhang J and Gu X (2022). Neuroinflammation-mediated mitochondrial dysregulation involved in postoperative cognitive dysfunction. *Free Radic Biol Med*. **178**: 134-146.

Ying J, Deng X, Du R, Ding Q, Tian H, Lin Y, Zhou B and Gao W (2024). Mitochondrial modulation treating postoperative cognitive dysfunction neuroprotection via DRP1 inhibition by Mdivi1. *Sci Rep*. **14**(1): 26155.

Zhang X, Li M, Yue Y, Zhang Y and Wu A (2023). Luteoloside prevents sevoflurane-induced cognitive dysfunction in aged rats via maintaining mitochondrial function and dynamics in hippocampal neurons. *Neuroscience*. **516**: 42-53.

Zhao R, Zhao D, Zhu X, Li F, Xiong P, Li S and Liu J (2024). The influence of miR-3149 on the malignancy progression of gastric cancer by negatively regulating CEACAM5. *J. Cancer Biomol. Ther.*. **1**(1): 1-10.

Zhou L, Pinho R, Gu Y and Radak Z (2022). The role of SIRT3 in exercise and aging. *Cells*. **11**(16): 2596.